Bifurcation Analysis of Power Systems with Tap Changer

Der-Cherng Liaw, Kuan-Hsun Fang and Chau-Chung Song

***Abstract*— A bifurcation analysis of nonlinear dynamics for electric power system with tap changer is presented in this paper. Based on a model of electric power system proposed by Dobson and Chiang (1988) with one extra tap changer added parallel to the local nonlinear power load, the saddle-node bifurcation and Hopf bifurcations are observed by treating the real power, reactive power and tap changer as system parameters. The occurrences of subcritical Hopf bifurcation and saddle-node bifurcation lead to the appearance of dynamic and static voltage collapses, respectively. These phenomena may generate the progressive decrease in voltage magnitude in electric power system.**

***Index Terms*— electric power system, bifurcation analysis, tap changer.**

I. Introduction

In the recent years, the study of voltage collapse phenomena in real-world electric power systems has attracted lots of attention [1]-[15]. It is due to the power systems facing growing load demands but with little addition of the power generation and transmission facilities. That leads the power systems to be operated near the stability limits. As the load demands become too heavy to offer, the magnitude of load voltage fall sharply to a very low level – that is the so-called "voltage collapse."

A practical power system is a large electrical network that containing components such as generators, loads, transmission lines and voltage controllers. In [2] and [3], Dobson and Chiang introduced a simple dynamical model for electric power systems, which consisted of a generator, a nonlinear load and an infinite bus. Based on this model, several results have been published regarding the nonlinear phenomena of electric power systems [7]-[9]. In addition, the occurrence of voltage collapse had been believed to be attributed to the existence of saddle-node bifurcation of electric power systems [4]-[5]. However, in the recent years, it has been shown that voltage collapse may arise from the existence of Hopf bifurcation, which is prior to the appearance of saddle-node bifurcation [13]-[15]. The effect of tap changer ratio on the nonlinear behavior of an electric power system has been studied for the large scale electric power networks [1] and [10]-[12]. However, no explicit disscussions have been proposed yet to analyze the dynamic behavior of electric power systems via the setting of tap changer ratio.

D.-C. Liaw is with the Department of Electrical and Control Engineering, National Chiao Tung University, Hsinchu 300, Taiwan, R.O.C. (e-mail: dcliaw@cc.nctu.edu.tw)

C.-C. Song is with the Department of Electrical Engineering, Chung Hua University, Hsinchu 300, Taiwan, R.O.C.

0-7803-8812-7/05/$20.00 ©2005 IEEE

In this paper, an extra tap changer is added to the nonlinear load of the power model [2]-[3] in parallel. The main goal of this paper is to determine the implications of the bifurcation behaviors for the voltage collapse phenomenon in the power system with tap changer. We focus on the nonlocal numerical study of the electric power system dynamics by treating the real power, reactive power and tap changer as system parameters. First, a dynamical model of a power system with tap changer dynamics is constructed. By adopting numerical values of [2], a numerical study of system stability and bifurcation characteristics with different setting of PQ load and tap changer ratio is achieved by using code AUTO [18].

II. Dynamical Equations of Electric Power Systems

In this paper, we focus on the study of the mathematical model proposed by Dobson and Chiang [2] and [3] for electric power systems. The main difference is that we add a voltage controller – tap changer to the original power system model as shown in Fig. 1. The model contains the infinity bus, the nonlinear load, the tap changer and the generator. The nonlinear load model includes a dynamic induction motor model with a constant PQ load in parallel. The dynamic induction motor model specifies the real and reactive power demands of the motor in terms of load voltage and frequency. The model of the load is supposed to be given by

$$P = P_0 + P_1 + k_{p\omega}\dot{\delta} + k_{pv}(V + T\dot{V}), \quad (1)$$

$$Q = Q_0 + Q_1 + k_{q\omega}\dot{\delta} + k_{qv}V + k_{qv^2}V^2, \quad (2)$$

where P_0 and Q_0 denote the constant real and reactive powers of the motor. In addition, P_1 and Q_1 represent the PQ load.

In the following discussion, we assume that the values of real power demand, reactive power demand and tap changer ratio can be varied. The parameter values of [2] are as adopted here. Let $x_1 = \delta_m, x_2 = \omega_m, x_3 = \delta$ and $x_4 = V$ where δ_m, ω_m, δ and V denote the generator phase angle, the generator phase angle velocity, the phase angle of the load voltage and the load voltage, respectively. We then have the following state equations.

$$\dot{x}_1 = x_2, \quad (3)$$

$$\dot{x}_2 = 3.3333(0.5642 - 0.05x_2 + \frac{5x_4}{n}\sin(0.0873 - x_1 + x_3)), \quad (4)$$

$$\dot{x}_3 = -33.3333(-1.3 - Q_1 + 2.8x_4 - x_4^2(10.0239 + \frac{4.981}{n^2}) + 20x_4\cos(0.0873 - x_3)$$

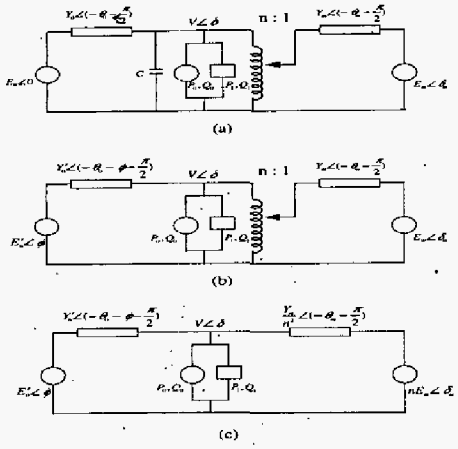

Fig. 1. Power system model.

$$+(\frac{5x_4}{n}\cos(0.0873+x_1-x_3))), \quad (5)$$

$$\begin{aligned}\dot{x}_4 = & -13.0719(-1.111x_4+0.84x_4^2-0.4(-1.3-Q_1\\ & -x_4^2(7.9239+\frac{4.981}{n^2})+20x_4\cos(0.0873-x_3)\\ & +\frac{5x_4}{n}\cos(0.0873+x_1-x_3))-0.03(-0.6-P_1\\ & +x_4^2(-1.7431-\frac{0.4358}{n^2})+20x_4\sin(0.0873-x_3)\\ & +\frac{5x_4}{n}\sin(0.0873+x_1-x_3))). \quad (6)\end{aligned}$$

Here, P_1, Q_1 and n denote the real power load, reactive power load and the tap changing ratio, respectively.

In the next section, we study the stability and bifurcation phenomena of the power system (3)–(6) via numerical approach.

III. Stability and Bifurcation Analysis

In the following discussion, we will consider Q_1 as a bifurcation parameter and to examine the effects of real power demand and tap changer ratio. First, we will consider the condition of $P_1 = 0$ and $n = 1$. Next, we will find the effect of real power demand. Finally, we will discuss the effect of tap changer.

A. Tap Changing Ratio $n = 1$

First, consider the case of which $P_1 = 0$ and $n = 1$, which is similar to the system proposed in [16]-[17]. Then by running code AUTO [18], we find that several kinds of bifurcation points occur. The locations of these bifurcation points are listed in Table I. Fig. 2 shows the equilibrium points and periodic solutions emerging from bifurcation points for the open-loop system (3)–(6), where

"——" (solid line) : stable equilibrium point,
"..." (dotted line) : unstable equilibrium point,
" * " (starred) : stable limit cycle, and
" o " (circle) : unstable limit cycle.

For simplicity, we define the following acronyms to be used in this paper.

1. HB1 : the first Hopf bifurcation point,
2. CFB : the cyclic fold bifurcation point,
3. PD1 : the first period doubling bifurcation point,
4. PD2 : the second period doubling bifurcation point,
5. HB2 : the second Hopf bifurcation point,
6. SNB : the saddle-node bifurcation point.

	δ_m (rad)	ω_m (p.u.)	δ (rad)	V (p.u.)
HB1	0.18624	0.0	−0.005037	1.086
HB2	0.21881	0.0	0.010831	0.93714
SNB	0.22327	0.0	0.01282	0.91841
CFB	0.63245	1.54473	0.13503	1.11565
PD1	0.61798	1.47118	0.14109	1.10555
PD2	0.28633	0.21901	0.36949	0.98176

TABLE I
LOCATION FOR BIFURCATION POINTS

	Q_1 (p.u.)	Transversality	β_2
HB1	10.89219	0.09936	0.09523
HB2	11.31728	−17.52886	−194.62732
SNB	11.32264	-	-
CFB	10.78072	-	-
PD1	10.8423	-	-
PD2	11.29447	-	-

TABLE II
PARAMETERS FOR BIFURCATION POINTS

In the course of computing a stationary branch, three critical points (HB1, HB2 and SNB) are detected as shown in Figure 2, at which the system changes stability. At two critical points, HB1 and HB2, a pair of complex conjugate eigenvalues cross the imaginary axis. At the last critical point SNB, one negative real eigenvalue cross the zero point and change to positive real eigenvalue. Thus, as depicted in Fig. 2, the stable operating point of the system becomes unstable prior to the fold bifurcation (SNB). In practical situation, the reactive power load Q_1 is increasing smoothly. So, we may say that the power system will occur voltage collapse before SNB. Thus, here we mainly consider the region between the two operating points HB1 and HB2. To show the satisfaction of Hopf bifurcation condition, the transversality condition (see, e.g., [16]) of the system is verified numerically in Table II. The eigenvalues of HB1 and HB2 are found to be $(\pm 3.7203j, -129.28, -14.619)$ and $(\pm 2.8985j, -94.069, -2.5864)$, respectively. By calculating the values of Floquet exponent β_2 (see definition, e.g., [16]), we have that HB1 is subcritical while HB2 is supercritical.

For convenience of reference, denote the values of Q_1 in Table II from HB1 to SNB by $Q_{11}, Q_{12}, ..., Q_{16}$, respectively. From Fig. 2, we know that for $Q_1 < Q_{11}$, the upper branch is stable. Now we consider the equilibrium points lying in the upper branch. Let Q_1 be increased, an unstable (or subcritical) Hopf bifurcation is encountered at HB1, since the corresponding parameter $\beta_2 > 0$ as presented in Table

II. As Q_1 is increased further, the equilibrium points regain stability at $Q_1 = Q_{15}$, where a stable (or supercritical) Hopf bifurcation point HB2 is encountered due to $\beta_2 < 0$. It is also observed from Fig. 2 that this stable equilibrium will merge with an unstable stationary branch and disappears at SNB as Q_1 increases.

In addition to the nominal equilibrium, we consider the periodic solutions born at the points between HB1 and HB2. Since HB1 is a subcritical bifurcation, the periodic solution branch from HB1 to CFB will be unstable limit cycles. At $Q_1 = Q_{12}$, the unstable periodic orbit turns to the right and gains stability. However, with the further increase of Q_1, the stable periodic orbit loses stability at the period doubling point PD1. At this bifurcation point, the previous periodic solution bifurcates to a new periodic orbit with twice of the period. If we keep tracing the old periodic orbit with increasing the value of Q_1, another period doubling bifurcation is found to occur at PD2. When it passes through the second period doubling point PD2, the periodic orbit gains stability again between the supercritical region between PD2 and HB2. Finally, the system oscillation is vanished at HB2.

According to the bifurcation theory, it is known that one way to have chaotic motion is through a sequence of period doubling bifurcations. On the parameter range between Q_{13} and Q_{14}, it is expected that there are further period doublings (not shown) just beyond PD1 and PD2 indicated in Fig. 2. This indicates there are two period doubling cascades, which will ultimately result in chaotic orbits. Indeed, one surmises there are an infinite number of periodic branches, with higher period, and paralleling the branch between PD1 and PD2. A typical chaotic behavior is shown in Fig. 5 (a).

B. The Effect of Real Power

Next, we will consider the effect of the real power P_1 under the condition of $n = 1$. Since the system (3)–(6) may undergo dynamic voltage collapse between HB1 and HB2 and static voltage collapse after SNB, we will now study the effect of real power load on the occurrence of both Hopf bifurcation and saddle node bifurcation. Figs. 3 and 4 show the locations of Hopf bifurcation points HB1 and HB2 and saddle node bifurcation point SNB in two-parameter (P_1 and Q_1) space with respect to different n, respectively. First, we consider the effect of P_1 on the pair of Hopf bifurcation points HB1 and HB2. It can be seen that the two points HB1 and HB2 move closer and closer to each other as P_1 increases. As P_1 increases further, HB1 merges with HB2 and then leading to disappearance. Thus, it is concluded that we might be able to eliminate the unstable region between HB1 and HB2 of the system (3)–(6) by increasing the value of P_1. Moreover, it is also observed from Fig. 3, we can anticipate the mergence of HB1 and HB2 by increasing n.

Now, we consider the effect of P_1 on the location of saddle node bifurcation point. From Fig. 4, we find that increasing P_1 will involve the saddle node bifurcation letdown. That means adding P_1 will anticipate the static bifurcation occurrence and induce the shortening of the stable region. Note that will contradict to the previous hope to eliminate Hopf bifurcation. It also can be seen that by increasing P_1, the Hopf bifurcation points (HB1 and HB2) will merge before saddle node bifurcation point SNB arise. Consequently, we can conclude that the optimum condition to stabilize the system by increasing P_1 is the vertex of the Hopf bifurcation point curve.

In Fig. 5, we can see the phenomenon of chaos. Figure 6 shows the time responses of Fig. 5, respectively. From Fig. 5 (a)–(e), it also demonstrates that the chaotic phenomenon can be eliminate by increasing P_1. These are conformity to all the above discussions. Moreover, Fig. 5 (f) shows the appearance of transient chaos. It can be seen that it is dangerous to the system.

C. The Effect of Tap Changer

After the discussion of the effect of real power load, in this subsection we will consider the effect of the tap changer under the situation of $P_1 = 0$. Similar to the previous discussion, we will discuss the effect of tap changer at both Hopf bifurcation and stationary bifurcation.

Fig. 7 shows the Hopf bifurcation points in the two-parameter (n and Q_1) space at different value of P_1. It can be seen that as n increases from 1, HB1 and HB2 almost increase in the same velocity. That is increasing n will postpone the occurrence of HB1 and HB2. However, when n increases further, the increasing velocity of HB2 slow down and it merges with HB1 leading to their disappearance. Thus, the unstable segment between HB1 and HB2 of the system (3)–(6) will shrinks and ceases by increasing n. Moreover, it also show that we can anticipate the mergence of HB1 and HB2 by increasing P_1, these agree the above discussions.

Secondly, we consider the effect of n on the appearance of the saddle node bifurcation point SNB. Fig. 8 shows the saddle node bifurcation curve with respect to different P_1. From Fig. 8, we find that the curve moves upward quickly at the beginning as n increases. But it begins to go downward after $n \simeq 2.3$. That is, we can't increase n infinitely to postpone the occurrence of voltage collapse. As n increases to a too large value, it will induce the shortening of the stable region.

To see more carefully about the effect of tap changer reverse action, we treat the tap changer ratio n as the primary parameter. Fig. 9 shows the voltage curves at $P_1 = 0$ as n increases. It can be seen that the voltage may be pulled down as n increases. Fig. 10 demonstrates the reverse action. Furthermore, we find that the increase of n will also result in the appearance of another saddle-node bifurcation. That is, as n increases to a large value, it will induce not only the shortening of the stable region but also the static voltage collapse. Moreover, Fig. 11 shows the chaotic phenomenon at $n = 1.001$. Comparing with Fig. 5 (a), we find that the transient chaos region moves upwards. Note that, there is a sticky problem when increasing n. As we know, the help of increasing n is to uplift the voltage such that we can prolong the stable region. However, the work space of voltage in the power system is required to be within $0.9p.u.$ to $1.1p.u.$ Although we can prolong the stable region by increasing n; nevertheless it may exceed the practical work region.

IV. Conclusions

In this paper, we focus on the nonlinear analysis of bifurcation phenomena for a power system with tap changer. The simulations demonstrate that the occurrence of bifurcations might lead to the voltage collapse of power system. It was found that the nominal operating point undergoes dynamic bifurcations prior to the static bifurcation to which voltage collapse has been attributed. Moreover, it was also found that in the power systems, bifurcation phenomena may happen, even in periodic orbits. Among the periodic bifurcations, the chaotic phenomena may exist between the period-doubling points of system equilibria. The effects of real power demand in PQ load and tap changer ratio on the existence of system equilibria were also obtained. The merging range of Hopf bifurcation can be shrunk or even eliminated by increasing the system parameters. Furthermore, the stable region of system equilibria can be enlarged by increasing the tap changer ratio.

ACKNOWLEDGMENTS

This research was partially supported by the Ministry of Education, Taiwan, R.O.C. under Grant: 91-E-FA06-4-4.

References

[1] S. Abe, Y. Fukunaga, A. Isono and B. Kondo, "Power system voltage stability," *IEEE Transactions on Power Apparatus and Systems*, Vol. PAS-101, No. 10, pp. 3830–3840, 1982.

[2] I. Dobson, H.-D. Chiang, J. S. Throp and L. Fekih-Ahmed, "A model of voltage collapse in electric power systems," *Proc. 27th IEEE Conference on Decision and Control*, Austin, Texas, Dec. 1988, pp. 2104–2109.

[3] H.-D. Chiang, I. Dobson, R. J. Thomas, J. S. Throp and L. Fekih-Ahmed, "On voltage collapse in electric power systems," *IEEE Transactions on Power Systems*, Vol. 5, No. 2, pp. 601–611, 1990.

[4] I. Dobson and H.-D. Chiang, "Towards a theory of voltage collapse in electric power systems," *Systems & Control Letters*, Vol. 13, pp. 253–262, 1989.

[5] H. G. Kwatny, A. K. Pasrija, and L. Y. Bahar, "Static bifurcation in electric power networks : loss of stability and voltage collapse," *IEEE Transactions on Circuits and Systems*, Vol. CAS-33, pp. 981–991, 1986.

[6] I. Dobson, H. Glavitsch, C.-C. Liu, Y. Tamura and K. Vu, "Voltage collapse in power systems," *IEEE Circuits and Devices Magazine*, Vol. 8, No. 3, pp. 40–45, 1992.

[7] V. Ajjarapu and B. Lee, "Bifurcation theory and it's application to nonlinear dynamical phenomena in an electrical power system," *IEEE Transactions on Power Systems*, Vol. 7, No. 1, pp. 424–431, 1992.

[8] H.-D. Chiang, C.-W. Liu, P. P. Varaiya, F. F. Wu and M. G. Lauby, "Chaos in a simple power system," *IEEE Transactions on Power Systems*, Vol. 8, No. 4, pp. 1407–1417, 1993.

[9] H. O. Wang, E. H. Abed and A. M. A. Hamdan, "Is voltage collapse triggered by the boundary crisis of a strange attractor?" *Proc. 1992 American Control Conference*, Chicago, June 1992, pp. 2084–2088.

[10] C.-C. Liu and K. T. Vu, "Analysis of tap-changer dynamics and construction of voltage stability regions," *IEEE Transactions on Circuits and Systems*, Vol. 36, No. 4, pp. 575–589, 1989.

[11] H. Ohtsuki, A. Yokoyama and Y. Sekine, "Reverse action of on-load tap changer in association with voltage collapse," *IEEE Transactions on Power Systems*, Vol. 6, No. 1, pp. 300–306, 1991.

[12] K. T. Vu and C.-C. Liu, "Shrinking stability regions and voltage collapse in power systems," *IEEE Transactions on Circuits and Systems–I: Fundamental Theory and Applications*, Vol. 39, No. 4, pp. 271–289, 1992.

[13] H. O. Wang, E. H. Abed, R. A. Adomaitis and A. M. A. Hamdan, "Control of nonlinear phenomena at the inception of voltage collapse," *American Control Conference*, San Francisco, California, June 1993, pp. 2071–2075.

[14] H. O. Wang, E. H. Abed, and A. M. A. Hamdan, "Bifurcations, chaos, and crises in voltage collapse of a model power system," *IEEE Transactions on Circuits and Systems–I: Fundamental Theory and Applications*, Vol. 41, No. 3, pp. 294–302, 1994.

[15] M. Yue and R. Schlueter, "Bifurcation Subsystem and Its Application in Power System Analysis," *IEEE Transactions on Power Systems*, Vol. 19, No. 4, pp. 1885–1893, 2004.

[16] E. H. Abed and J.-H. Fu, "Local feedback stabilization and bifurcation control, I. hopf bifurcation," *System & Control Letters*, Vol. 7, pp. 11–17, 1986.

[17] E. H. Abed and J.-H. Fu, "Local feedback stabilization and bifurcation control, II. stationary bifurcation," *System & Control Letters*, Vol. 8, pp. 467–473, 1987.

[18] E. Doedel, *AUTO 86 User Manual*, Computer Science Dept., Soncordia Univ., Jan. 1986.

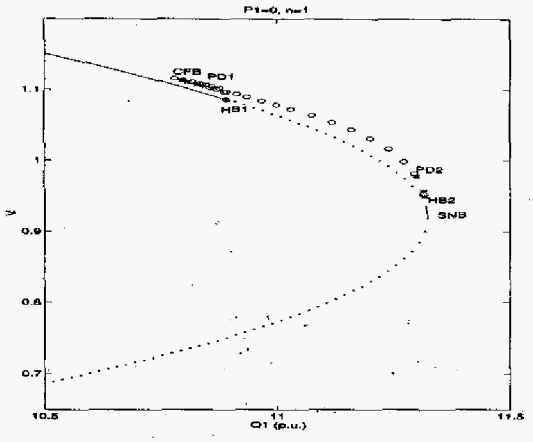

Fig. 2. Bifurcation diagram with respect to Q_1.

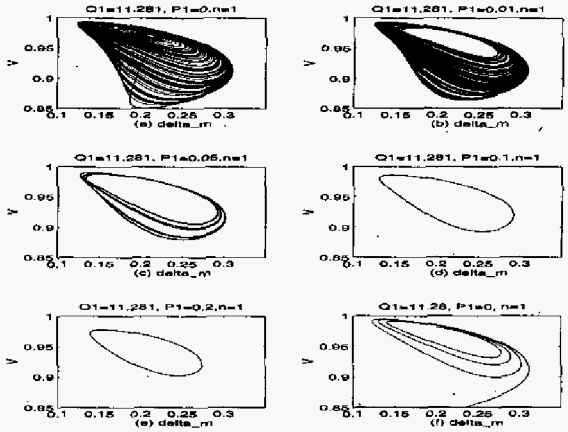

Fig. 5. Phase plane plot of chaos at $X_0 = [0.2, 0.2, 0.04, 0.98]$.

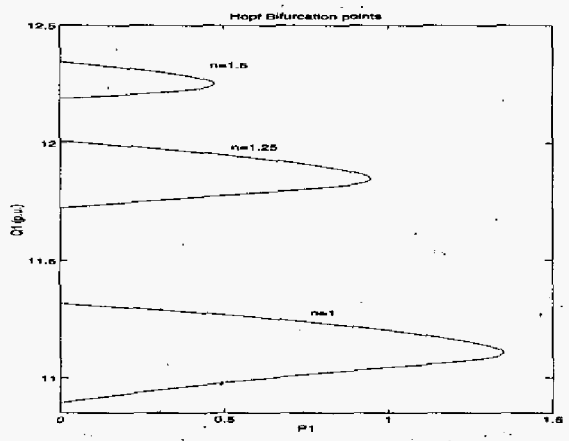

Fig. 3. Hopf bifurcation curves in (P_1,Q_1) space.

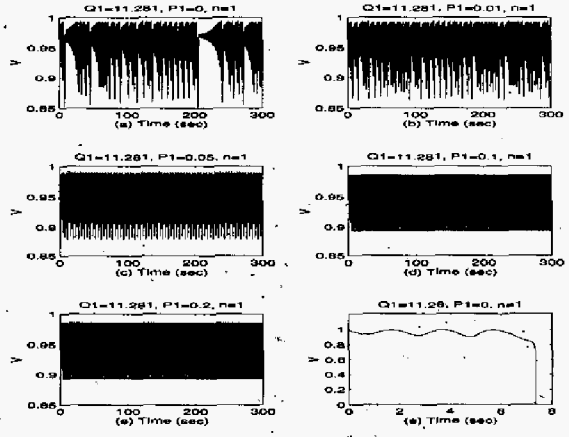

Fig. 6. Time domain plot of chaos at $X_0 = [0.2, 0.2, 0.04, 0.98]$.

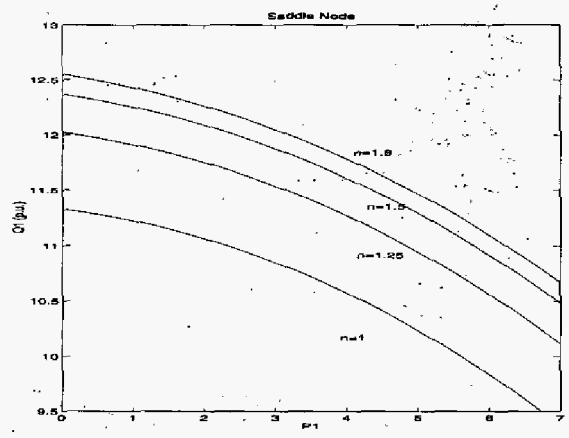

Fig. 4. Saddle node bifurcation curves in (P_1,Q_1) space.

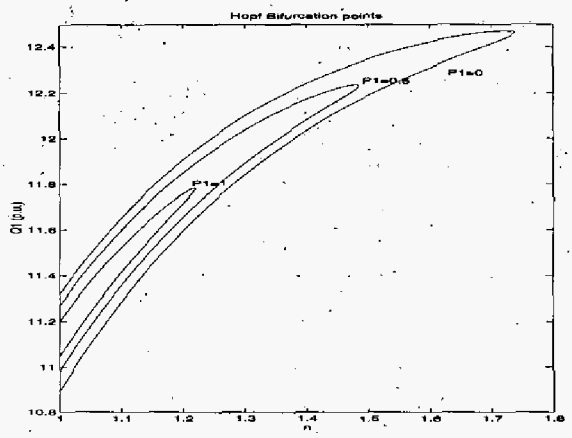

Fig. 7. Hopf bifurcation curves in (n,Q_1) space.

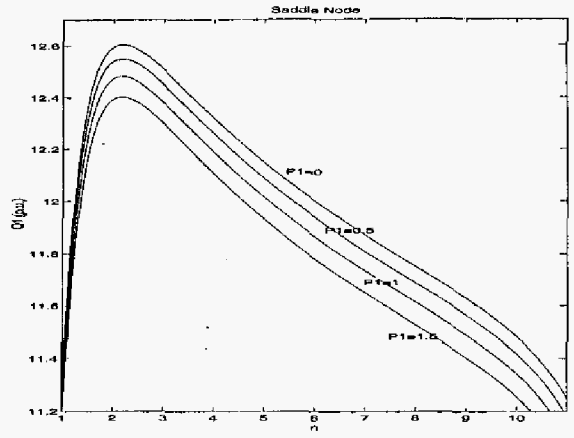

Fig. 8. Saddle node bifurcation curves in (n,Q_1) space.

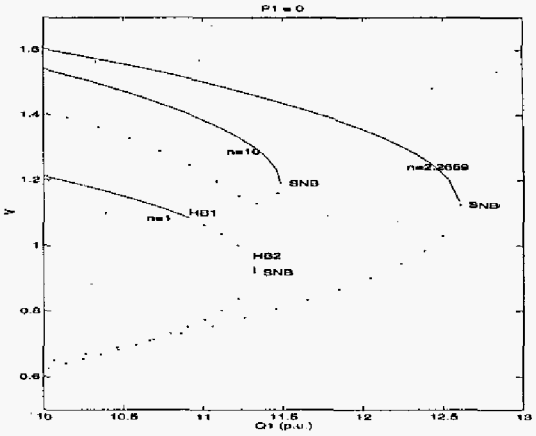

Fig. 10. Reverse action of the electric power system due to the variation of tap changer ratio.

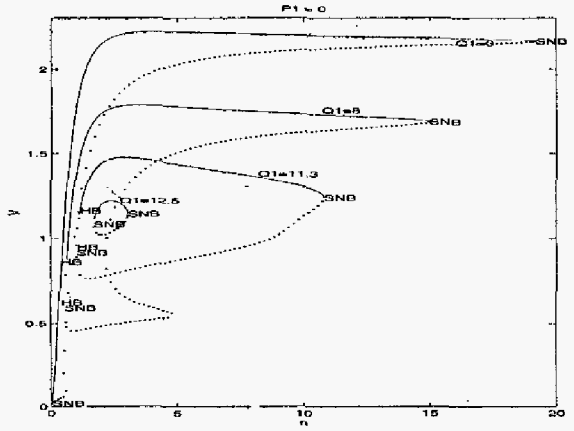

Fig. 9. Reverse action of tap changer with $P_1 = 0$.

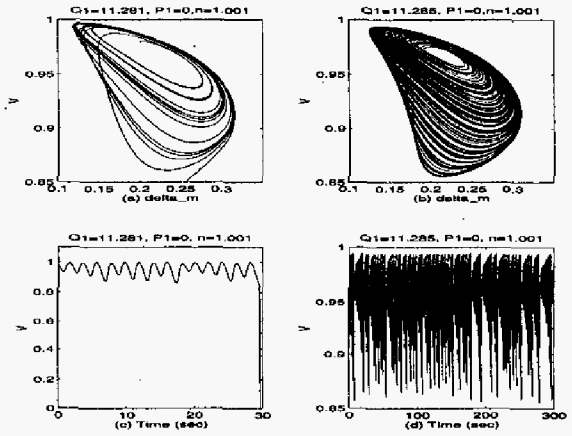

Fig. 11. Phase plane plot of chaos at $X_0 = [0.2, 0.2, 0.04, 0.98]$.